FULL-SCALE REINFORCED CONCRETE SLABS WITH EXTERNAL REINFORCED POLYMER: FIELD TEST AND NUMERICAL COMPARISON

RICARDO CASTEDO[1*], ANASTASIO P. SANTOS[1†], CARLOS REIFARTH[1‡],
MARÍA CHIQUITO[1§], LINA MARIA LÓPEZ[1**], ALEJANDRO PÉREZ-CALDENTEY[2,3††],
SANTIAGO MARTÍNEZ-ALMAJANO[4] & ALEJANDRO ALAÑÓN[5‡‡]
[1]Departmento de Ingeniería Geológica y Minera, Universidad Politécnica de Madrid, Spain
[2]Departmento de Mecánica de Medios Continuos y Teoría de Estructuras,
Universidad Politécnica de Madrid, Spain
[3]FHECOR Consulting Engineers, Spain
[4]Escuela Politécnica Superior del Ejército, Spain
[5]Escuela Politécnica Superior de Ávila, Universidad de Salamanca, Spain

ABSTRACT

Numerical simulation of reinforced concrete (RC) slabs with the addition of an external reinforced polymer (FRP) have been developed and compared with full scale real tests. The size of the slabs was 4.4 x 1.46 m, with a span of 4 m, and a thickness of 15 cm. The slabs were built using concrete of class C25/30, and B500C reinforcing steel. Seven tests were conducted, one at a scaled distance of 0.83 m/kg$^{1/3}$, three at a scaled distance of 0.42 m/kg$^{1/3}$, and three at 0.21 m/kg$^{1/3}$. For the biggest scaled distance, the slab had no extra reinforcement. In the other two cases one of the slabs had no extra reinforcement, while the other two tests were performed with carbon fibre reinforcement (CFRP) and E-glass fibre reinforcement (GFRP) located on the face opposite to the blast. Numerical simulation was performed with LS-DYNA software. The study elements (concrete, steel and reinforcement) have been simulated in a Lagrangian formulation with solid elements, beam elements and shells, respectively. Three concrete models have been used and compared: CSCM, MAT72-R3 and RHT. As for the explosive, the CONWEP-based Load Blast Enhanced (LBE) card was used. Reinforcement with CFRP resulted in a generally reduced damage area on both surfaces. All models show a good correlation with the test results and a non-destructive damage estimation technique when comparing them in terms of damage area.

Keywords: LS-DYNA, blast tests, non-destructive technique, CSCM, RHT, LBE.

1 INTRODUCTION

Terrorist acts have unfortunately increased worldwide over the last century, but especially in the west and against civilian populations the use of improvised explosive devices (IEDs) has multiplied with a total of 11,971 attacks recorded between the years 2010 and 2020 alone [1]. Many of these attacks caused damage to structures (pillars, slabs, or beams) or their enclosures or cladding (curtain walls, bricks, tiles, etc.). The main problems derived are two, the first one a possible collapse of the structure and the consequent increase of victims; the second problem are the projections of materials that can cause serious injuries and even death. To better understand their performance and therefore improve the way to protect them,

* *http://orcid.org/0000-0002-5725-6272*
† *http://orcid.org/0000-0003-2708-9378*
‡ *https://orcid.org/0000-0003-2677-5421*
§ *http://orcid.org/0000-0003-2207-6674*
** *http://orcid.org/0000-0001-6250-0893*
†† *https://orcid.org/0000-0002-8575-1860*
‡‡ *https://orcid.org/0000-0003-3509-5831*

WIT Transactions on The Built Environment, Vol 209, © 2022 WIT Press
www.witpress.com, ISSN 1743-3509 (on-line)
doi:10.2495/HPSU220121

numerous studies have focused on the field test and numerical simulation of a structural element with different IEDs and various reinforcements (external or internal). The problem of many of these works is that for budget reasons, limitations in the explosive loads, excessive complexity (in simulations or handling the structural elements), tests are carried out on a small scale with the limitations that this entails when generalizing the conclusions (scale factor) [2].

The ideal would be to study the structures in their "real" dimension, but this is a complicated task and, in many cases, unrealistic due to mentioned limitations. There are some publications on this subject, such as the work by Bermejo et al. [3], which analyses the collapse of a two-span, three-story full-scale structure in the face of the sudden demolition of a central column; or the work by Kernicky et al. [4]. A good summary of different progressive collapse of reinforced concrete structures can be found in the recent work of Alshaikh et al. [5]. It is more common to find works on structural elements such as slabs [6], [7], beams-columns [8], [9], or walls [10], [11]. Of these, the vast majority are on a reduced scale, but there are some publications that present results on a real scale. Focusing on the slabs we can highlight among others the work of Castedo et al. [12] that focuses on the simulation of small loads with smooth particle hydrodynamics (SPH) and validates it with real tests of full-scale slabs; or the work of Ruggiero et al. [13] that performs tests with three full-scale slabs and validates the numerical models based on measured pressure and acceleration to then expand the type of models to be performed. The variety of reinforcements to be used for the improvement of structural elements, especially concrete, is very important and increasingly creative, but it is easy to classify between internal reinforcements (added to the matrix) and external reinforcements (outside the concrete). As an example, two recently published state-of-the-art papers cover an important variety of techniques, materials, and application examples [14], [15].

The analysis and comparison of results is usually based on three main aspects: analytical models, numerical models, and non-destructive techniques (NDTs); in addition to the immediate results measured in the tests, such as pressures, accelerations, velocities, or deformations. Analytical models consist of a sequence of formulas that, once adjusted, predict in a more or less simple way some variable of interest such as deformation, deflection, etc. [16]. Numerical models can be of different types depending on how the simulation of the blast load and the structural element is approached. If the load is simulated explicitly (geometry and equation of state), SPH [12] or Arbitrary–Lagrangian–Eulerian (ALE) [17] methods can be used. If the load is simulated using the TNT equivalent, the technique based on numerous blast test (load blast enhanced (LBE)) can be applied [18]. Structural elements can be simulated in the same way with solid elements without considering the surrounding air (Lagrangian or SPH) [19] or taking it into account with ALE [20]. It seems obvious that SPH or ALE techniques involve more computational time and resources but depending on the case, their characteristics are basic for a good and useful simulation. Regarding the NDTs there are a lot of different options depending on the material characteristics, size, or conservation state [21]. However, all these techniques are used to provide reproducible measures of material quality (i.e., concrete) in a specimen (or even a structure) without causing an extra damage to the element or the structure from which it is taken.

In this work, seven real-size RC slabs (in some cases with external reinforcement) against near detonations are presented and compared with numerical simulations using LS-DYNA software version 971-R11 and a non-destructive damage evaluation developed by the working team [22].

2 EXPERIMENTAL TESTS

Seven tests were conducted during 2019 at "La Marañosa" a technological centre of the National Institute of Aerospace Technology (INTA). Some of the most important test parameters are listed in Table 1. It should be noted that the S3 test was performed twice due to minor problems with the measuring equipment during the first trial.

Table 1: Test details.

Test #	Reinforcement	Scaled distance ($m/kg^{1/3}$)	Equivalent mass TNT (kg)	Charge height (m)
S1	None	0.83	1.74	1
S2	None	0.42	13.05	1
S3	Carbon	0.42	13.05	1
S4	Glass	0.42	13.05	1
S5	None	0.21	13.05	0.5
S6	Carbon	0.21	13.05	0.5
S7	Glass	0.21	13.05	0.5

The size of the slabs was 4.40 × 1.46 × 0.15 m and they were placed on concrete supports (2 × 1.2 × 0.90 m long, wide, high) covered with steel plates. The test S1 was designed to test the measuring equipment and to validate the numerical models, for these reasons the explosive mass was low. The shape of the explosive charge, for the high charge tests, could be defined as something between cube, cylindrical and bag following the UFC [23]. The charge was hanged on a rope for the trial at 1 m distance, while it was placed on top of a piece of polystyrene in the tests at 0.5 m. To estimate the TNT equivalent mass of the dynamite used, a peak pressure equivalent of 0.86 was applied [24]. See Fig. 1 for a general view of the slabs and details of the charge used.

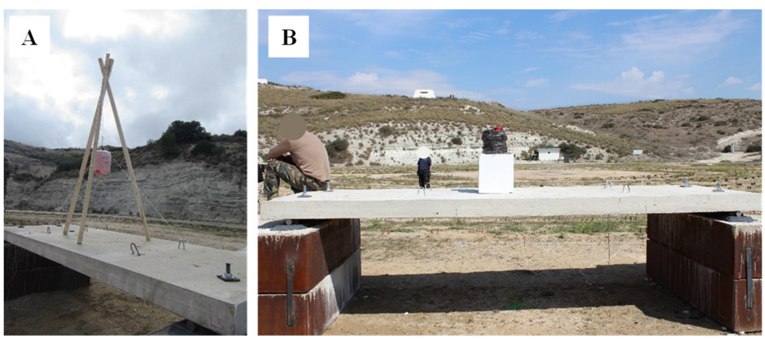

Figure 1: (A) Charge at 1 m; and (B) Charge at 0.5 m.

The properties of the concrete used in all the slabs are density (2,300 kg/m^3), uniaxial compressive strength (UCS) (25 MPa) and maximum aggregate size (0.02 m). The steel reinforcement was designed separately from the bottom (opposite face of the blast) and top (face that directly receives the blast). The 12 mm bars at the bottom were spaced 150 mm apart in both directions, while 10 mm bars at the top were spaced twice as far apart as on the other side. The steel used was the usual B-500 S construction steel. The properties have been extracted from the standard RC 1247/2008 – EHE-08 national design code based on EN-1992 [25]. These are the density (7,850 kg/m^3), Young's modulus (200 GPa), tangent modulus (20 GPa), yield strength (500 MPa) and Poisson's ratio (0.3).

In one case the RC slab was externally reinforced with carbon fibre (CFRP), in other, the slab was reinforced with E-glass fibres (GFRP). The same methodology has been followed on both scaled distances, first the non-external reinforced slab was tested, then the carbon one and finally the glass one. To ensure the proper functioning of the reinforcements and their solid union with the concrete, the carbon fibre was impregnated with an epoxy resin-based adhesive of thixotropic consistency, while the fibre glass was glued with a polyurethane-based adhesive. The main properties of the fibres are shown in Table 2.

Table 2: Properties of the carbon and glass fibres [19].

Property	Units	Carbon	Glass
Density	kg/m^3	1830	2000
Young modulus	GPa	252	42
Shear modulus	GPa	4.8	3.9
Elongation at failure	%	1.8	4
Poisson's ratio	–	0.3	0.285
Compression strength, principal direction	GPa	0.298	0.1129
Tensile strength, principal direction	GPa	2.93	1.62
In-plane shear strength	GPa	0.0845	0.0308

3 NUMERICAL MODEL

The 3D numerical models developed in this work are based on the use of LBE for the explosive loading, while the slab concrete, steel reinforcement and fibre reinforcement in a Lagrangian technique. The concrete has been simulated with solid elements (156936 elements), the steel reinforcement with beam elements (7,024 elements), and the fibres with shells of thickness equal to the real fibres, i.e., 1 mm (16,614 elements). Despite the importance of mesh convergence, 18 × 18 × 18 mm and 50 mm meshes have been used in this work for the solid and beam elements, respectively. An 18 × 18 mm mesh has been used for the shell (fibres), as in the solid elements, to have coincident nodes. These data are based on previous works already published by Castedo et al. [12], Reifarth et al. [19] and Alañón et al. [26]. It should be noted that the model has been made in a complete manner, without taking advantage of any of the symmetries, due to the absence of one of the reinforcing bars (see Fig. 2). This was detected once the tests were done and due to the spalling of the concrete that left the reinforcement visible. See Reifarth et al. [19] for more details.

In this work, three different concrete models have been used: the Continuous Surface Cap Model (MAT_159-CSCM_concrete), the Riedel–Hiermaier–Thoma (MAT_272-RHT), and the Karagozian and Case (MAT72-R3). Three material models are tested due to the influence of the numerical model, and therefore, of the mathematical treatment of the material characteristics. Furthermore, there is no agreement on the use of one or the other model as the optimal solution. CSCM was developed to simulate roadside safety simulations and was created by the U.S. Federal Highway Administration [27]. RHT was designed to simulate the concrete behaviour exposed to blast loads [28], as well as the MAT72-R3 [29]. Despite their disparate origins, all three models use three failure surfaces corresponding with the elastic limit (yield surface), strength (maximum surface) and failure (residual surface). These three material models have been chosen since they have reduced data input and basically work

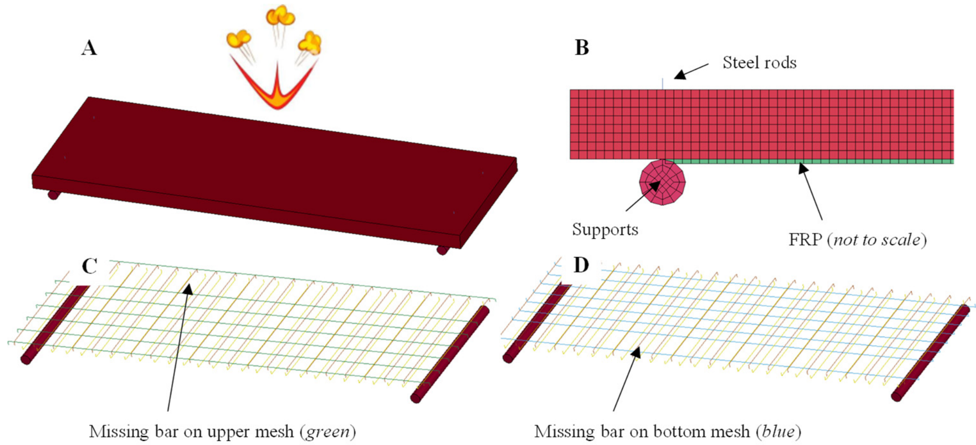

Figure 2: Details of LS-DYNA slab models. (A) Full model; (B) Details of the support and FRP modelling; (C) Longitudinal top and transverse (top = brown and bottom = yellow) steel reinforcement; and (D) Longitudinal bottom and transverse (top = brown and bottom = yellow) steel reinforcement.

with the introduction of UCS, density, and aggregate size. The required parameters, in all cases, are mentioned in Section 2, in the absence of the erosion parameters ERODE (CSCM) and EPSF (RHT). The former is left with its default value (1.05), while for the latter a value of 0.50 comparable to that used by the CSCM is used. Material MAT72-R3 has no damage parameter, although some researchers use the ad-hoc *MAT_ADD_Erosion criterion, it is not the case in this work.

For the incorporation of steel, the piecewise linear plasticity (MAT_24-PLP) model has been chosen. An elasto-plastic behaviour is described with this material model including the strain rate influence on material strength. The stress–strain relation is defined as a bilinear curve controlled by the tangent modulus. The failure is reached by effective plastic strain (7.5%). The parameters are specified in Section 2. One of the characteristics of an event like this is the fast speed at which it occurs, that allows us to reproduce the concrete–steel behaviour as a "solidary" element and incorporate it into the model with the constrained Lagrange in solid tool [30].

The material model called laminated composite fabric (MAT_058) has been used to describe the fibres (carbon (CFRP) and E-glass (GFRP)). Failure criteria is based on Hashin's theory [31]. The failure limit must be defined based on the failure surface selected of the fourth available options, with the smooth failure surface being the final choice after several trials. An erosion parameter equal to –0.55 has been applied after intensive calibration (more details of the FRPs modelling [19]). Material properties are listed in Section 2. The contact with the concrete has been defined using merging nodes (i.e., perfect bond), both elements have the same element size (more details in Reifarth et al. [19]).

In this case the explosive charge has been simulated using its TNT equivalent mass (Table 1) and implemented with the load blast enhanced (LBE) card. Using this card, in addition to the explosive mass, the type of charge, the coordinates of its centre and the face of the slab receiving the explosion must be introduced.

4 NON-DESTRUCTIVE DAMAGE ASSESSMENT (NDDA)

Among the many non-destructive techniques for analysing the condition of materials, here we use a cheap, simple, fast, and effective technique such as the Schmidt hammer. This tool is usually used to estimate the UCS of a material (through the rebound index), in this case concrete, provided that the reinforcement is deep enough (about 5 cm) so as not to affect the results. In this work, the hammer rebound index is used directly, without obtaining the necessary ratios for the estimation of the UCS.

The methodology consists of the creation of small measuring stations with 12 points, six of which are used to measure before the test and six to measure after. The medians of these measurements (*Pbt* (medians before the test); *Pat* (medians after the test)) are compared with the Wilcoxon rank-sum test and if the difference is significant at 95%, the measuring station is considered to have had a reduction in the rebound value. The damage (d_H) is calculated as follows for points with significant difference:

$$d_H = 1 - \frac{Pat}{Pbt}. \tag{1}$$

This parameter can vary between zero (for when the differences are not significant) and one (for when the differences are significant and the "damage is total"). In each slab there are 19 measuring stations distributed according to Fig. 3. To complete the analysis, a mesh of 200 points is created and a damage map is calculated using a triangle based cubic interpolation in MATLAB. For a better assessment of the damage data, and to avoid the heterogeneity of the measurement points, the mean value of the interpolated data is extracted (d_{200}) and used for comparison. See López et al. [22] for detailed information.

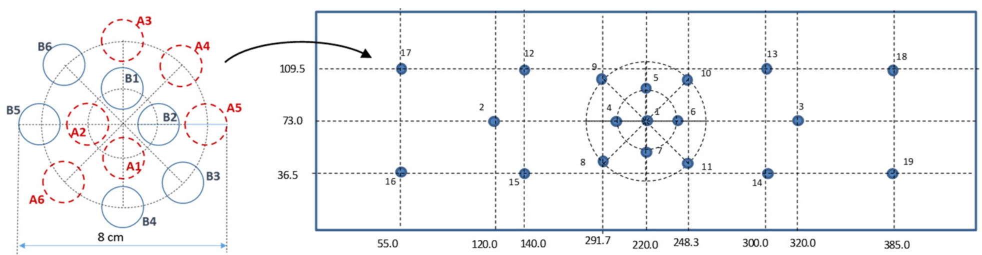

Figure 3: Detail of one of the stations with the six points before (blue) and after (red) the test and location of rebound index measurement stations (19) with the Schmidt hammer. Units in cm.

5 RESULTS AND DISCUSSION

All cases, except the first one, will be analysed according to the scaled distance and based on surface damage area, numerical damage area and non-destructive damage area, see Table 1 for more details. The surface damage area (d_A) is measured by direct test results and can be defined as the eroded area for each surface of the slab divided by the total area of that surface. The numerical damage area (d_{NA}) is measured in the numerical models and calculated as the ratio of the area of damaged elements and the total area for each surface. The non-destructive damage area is extracted from the interpolation maps created in MATLAB and referred as d_{200}, see previous section for details.

5.1 Fitting test (S1).

In this low load test, it was possible to measure the slab acceleration and shock wave pressure without damaging the measuring equipment. This allows us to compare these data with the generated models. The pressure was measured at a radial distance from the load of 1 m, as was done for the acceleration, i.e. 1 m from the centre of the slab. The pressure measured in the field was 2.01 MPa, while the pressure applied with the LBE card is 1.98 MPa, a minimum error of 1.5%. The acceleration measured in the field was equal to 1028.6 g, while the one provided by the CSCM model was 975.53 g (a difference of –5.16%), the RHT was 1,080.10 g (5.01%) and the MAT72-R3 was 1,126.73 (9.54%). Acceleration values are quite good in two of the three cases and acceptable in a third (MAT72-R3). However, as shown in Fig. 4, the damage surfaces of the models are good in CSCM, acceptable in RHT and poor in MAT72-R3. Note that strain rates could only be measured in numerical models and not in tests. For these reasons the MAT72-R3 material is discarded for further analysis. Notice that, in Fig. 4, d_{200} map corresponding to slab S1 is not drawn since the damage obtained in this test was 0%.

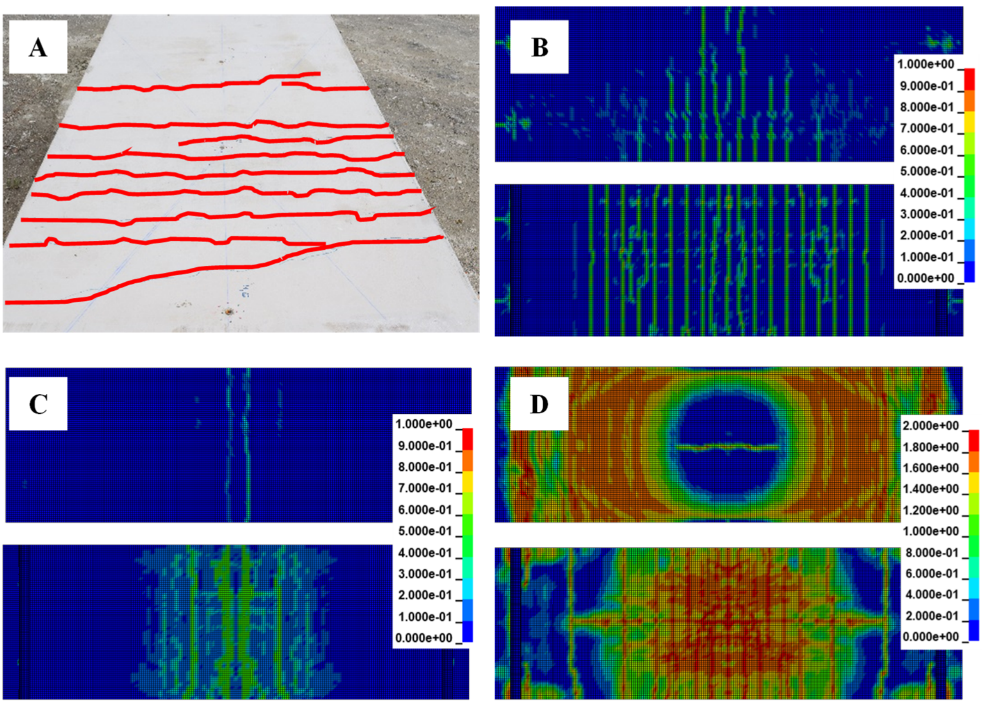

Figure 4: Results for slab S1. (A) Bottom damage; (B) Top and bottom damage with CSCM; (C) Top and bottom damage with RHT; and (D) Top and bottom damage with MAT72-R3.

5.2 Slabs with no external reinforcement (S2, S5).

Considering the results obtained, the simulations of slabs S2 and S5 have been performed with CSCM and RHT. Table 3 shows the damage area values obtained from the tests and the models, in addition to the d_{200} value extracted from the Schmidt hammer maps. The RHT model is not able to reproduce the damage in slab S2 on either side. Given this result, and as slab S5 also shows significant errors especially on the bottom face, the RHT model is discarded for the following simulations with FRPs.

Table 3: Damaged area for slabs S2 and S5 without fibres.

Slab	S	d_A (%)	d_{NA} CSCM (%)	Rel. dif. (%)	d_{NA} RHT (%)	Rel. dif. (%)	d_{200} (%)
S2	T	3.38	4.20	13.80	*	–	18.77
	B	10.34	10.83	4.77	*	–	–
S5	T	8.19	8.48	3.55	9.19	12.17	27.69
	B	18.62	17.63	–5.35	8.82	–52.62	–

Note: S = the surface; T = Top; B = Bottom. * indicates that there is no damage in the model.

As for the damage map generated from NDDA, the S2 slab has a centralized and transversal damage on the surface of the slab that receives the explosion (see also Fig. 5). In slab S5 the damage is 10% higher and is focused on the centre of the slab. Although the damage is presented in an asymmetrical way that may indicate that the load was not perfectly located in the centre or some heterogeneity in it.

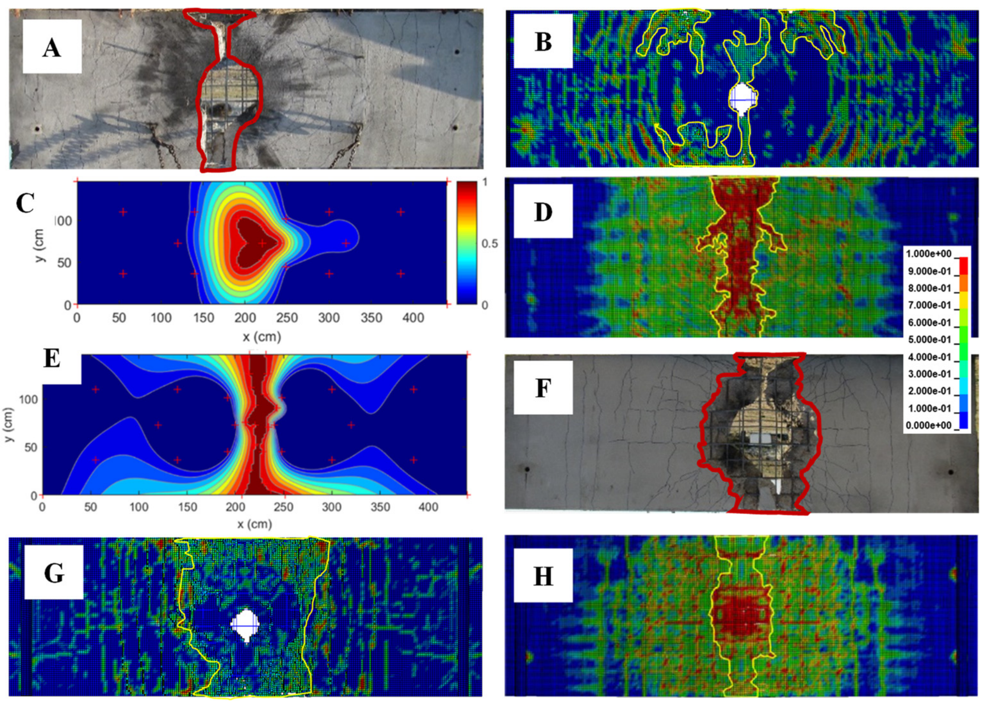

Figure 5: (A) Top damage S5; (B) Top damage with CSCM S5; (C) Damage map from NDDA S5; (D) Top damage with MAT72-R3 S5; (E) Damage map from NDDA S2; (F) Bottom damage S5; (G) Bottom damage with CSCM S5; and (H) Bottom damage with MAT72-R3 S5.

5.3 Scaled distance equal to 0.42 m/kg$^{1/3}$ (S3, S4).

Again, the simulation values are quite good, not exceeding 15% differences with the CSCM model and both types of fibres (see Table 4). In general, the model underestimates the damage area values, except in the case of the slab reinforced with glass fibre. Comparing both results with the S2 slab (without reinforcement), it is observed that the damage on the top face is practically the same, but on the bottom face it is reduced by about 4%–5%.

Table 4: Damaged area for slabs S3 and S4.

Slab	Reinforcement	S	d_A (%)	d_{NA} CSCM (%)	Rel. dif. (%)	d_{200} (%)
S3	Carbon	T	3.27–5.45	3.04	–6.93	19.33–21.26
		B	6.71–6.96	6.43	–7.54	–
S4	Glass	T	3.89	3.66	–6.02	17.85
		B	5.78	6.52	12.72	–

Note: S = the surface; T = Top; B = Bottom.

With respect to the damage maps (d_{200}), the values obtained are much higher than those measured in the test and in the numerical models (see Table 4 and Fig. 6). This is because the data comes from a damage not only superficial, but corresponding to a depth of about 3/5 cm. Therefore, it can detect a loss of resistance that does not seem to be estimated at all with the numerical model. There would be an exception to this, and that is if green areas (with intermediate damage in the model) are considered as damage as is done with the damage maps. In any case, and even if the value of the area were similar, they do not occur in the same areas and with the same pattern.

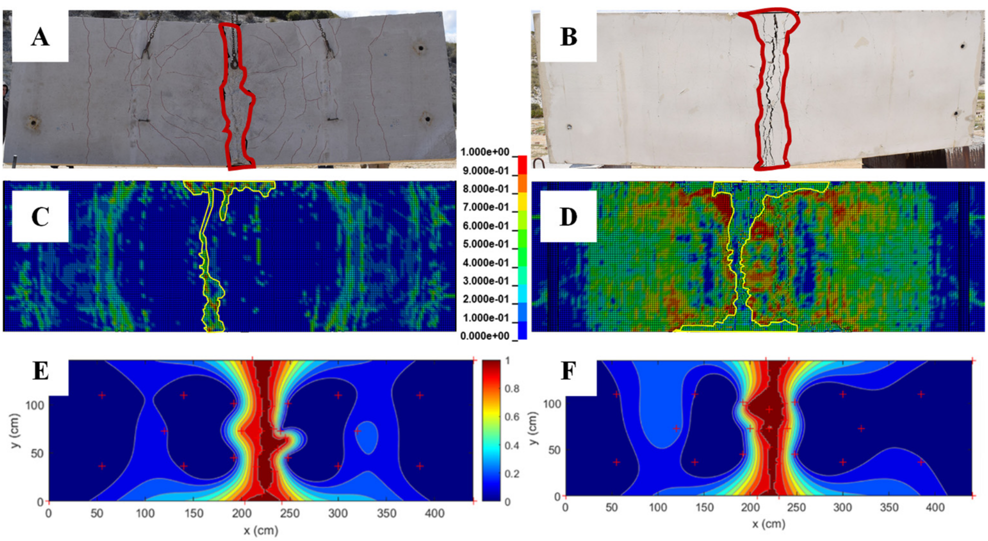

Figure 6: (A) Top damage slab S4; (B) Bottom damage slab S4; (C) Top damage with CSCM S4; (D) Bottom damage with CSCM S4; (E) Damage map from NDDA S4; and (F) Damage map from NDDA S3.

WIT Transactions on The Built Environment, Vol 209, © 2022 WIT Press
www.witpress.com, ISSN 1743-3509 (on-line)

5.4 Scaled distance equal to 0.21 m/kg$^{1/3}$ (S6, S7).

The damage in the CFRP test (S6) was reduced in comparison with the S5 on both sides (Table 5). However, in the test S7 with the CFRP the top face damage was also reduced but the bottom increased. This is because the glass fibre was not well bonded to the concrete and became detached during the test, dragging with it pieces of concrete that increase the damage surface although not as proper spalling.

Table 5: Damaged area for slabs S6 and S7.

Slab	Reinforcement	S	d_A (%)	d_{NA} CSCM (%)	Rel. dif. (%)	d_{200} (%)
S6	Carbon	T	7.83	7.54	–3.64	28.22
		B	16.78	19.59	16.74	–
S7	Glass	T	7.63	6.96	–8.72	28.93
		B	22.48	22.85	1.66	–

Note: S = the surface; T = Top; B = Bottom.

The numerical model continues to show results very close to reality, with a maximum difference of 15%. The damage maps (d_{200}) continue to have similar values in all three cases (S5, S6 and S7) at the same scaled distance of 0.21 m/kg$^{1/3}$ (Fig. 7). This shows that it can be used to detect the non-visual surface damage, as it is consistent with the calculated damage areas, but they do not allow to differentiate whether a reinforcement improves the constructive element or not (at least on the face receiving the detonation).

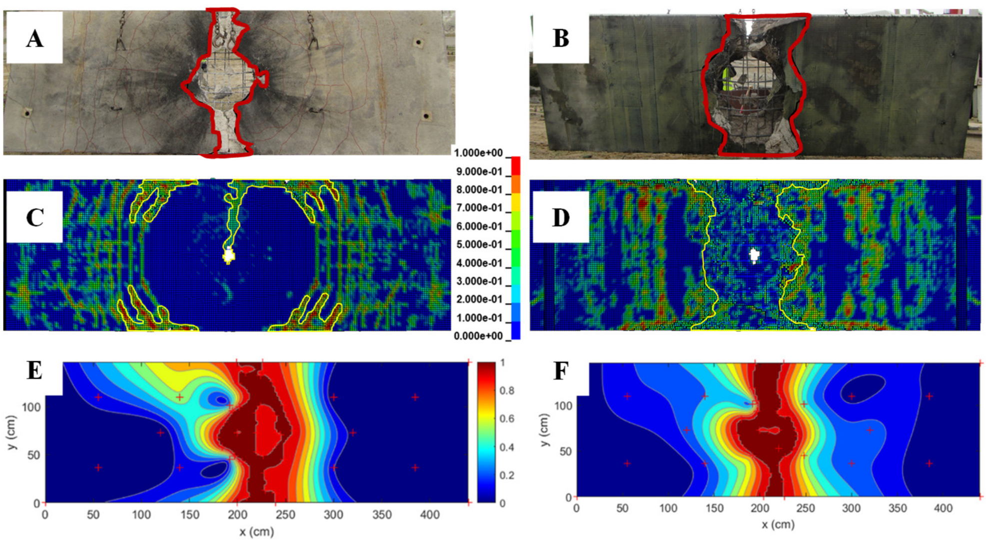

Figure 7: (A) Top damage slab S6; (B) Bottom damage slab S6; (C) Top damage with CSCM S6; (D) Bottom damage with CSCM S6; (E) Damage map from NDDA S6; and (F) Damage map from NDDA S7.

6 CONCLUSIONS

This work allows us to conclude the following:

- reinforcement with carbon or glass fibres improves blast performance especially at intermediate scaled distances, however, a critical point seems to be the bond between the fibres and the concrete;
- damage maps created using Schmidt hammer data respond well to changes in scaled distance, but less so to reinforcement types. However, although more testing is needed, they appear to be a useful tool for quick and reliable analysis at the surface of the material after a detonation;
- 3D numerical models with LS-DYNA software and the appropriate use of material models allow simulations very close to the real results;
- from the above it follows that, given the high cost of real tests, if reliable and calibrated numerical models exist, many more scenarios can be studied at a reduced cost.

ACKNOWLEDGEMENTS

The Centre for Industrial Technological Development (CDTI) funded the PICAEX project, a consortium between TAPUSA, MAPEI and FHECOR, with the collaboration of the Universidad Politécnica de Madrid. The authors would like to thank the staff of “La Marañosa” (INTA) for their support in the trials.

REFERENCES

[1] Overton, I., Davies, R. & Tumchewics, L., Improvised explosive devices: Past, present and future. *Action on Armed Violence*, 2020.

[2] Badshah, E., Naseer, A., Ashraf, M., Shah, F. & Akhtar, K., Review of blast loading models, masonry response, and mitigation. *Shock and Vibration*, 2017.

[3] Bermejo, M., Santos, A.P. & Goicolea, J.M., Development of practical finite element models for collapse of reinforced concrete structures and experimental validation. *Shock and Vibration*, 4636381, 2017.

[4] Kernicky, T.P., Whelan, M.J., Weggel, D.C. & Rice, C.D., Structural identification and damage characterization of a masonry infill wall in a full-scale building subjected to internal blast load. *Journal of Structural Engineering*, **141**(1), D4014013, 2015.

[5] Alshaikh, I.M., Bakar, B.A., Alwesabi, E.A. & Akil, H.M., Experimental investigation of the progressive collapse of reinforced concrete structures: An overview. *Structures*, **25**, pp. 881–900, 2020.

[6] Kumar, V., Kartik, K.V. & Iqbal, M.A., Experimental and numerical investigation of reinforced concrete slabs under blast loading. *Engineering Structures*, **206**, 110125, 2020.

[7] Foglar, M., Hajek, R., Fladr, J., Pachman, J. & Stoller, J., Full-scale experimental testing of the blast resistance of HPFRC and UHPFRC bridge decks. *Construction and Building Materials*, **145**, pp. 588–601, 2017.

[8] Liu, Y., Yan, J.B. & Huang, F.L., Behavior of reinforced concrete beams and columns subjected to blast loading. *Defence Technology*, **14**(5), pp. 550–559, 2018.

[9] Thai, D.K., Nguyen, D.L., Pham, T.H. & Doan, Q.H., Prediction of residual strength of FRC columns under blast loading using the FEM method and regression approach. *Construction and Building Materials*, **276**, 122253, 2021.

[10] Chiquito, M., Castedo, R., Santos, A.P., López, L.M. & Pérez-Caldentey, A., Numerical modelling and experimental validation of the behaviour of brick masonry walls subjected to blast loading. *International Journal of Impact Engineering*, **148**, 103760, 2021.
[11] Chiquito, M., Clubley, S.K., Martinez-Almajano, S., Santos, A.P., Castedo, R. & Lopez, L.M., Numerical and experimental study of unreinforced brick masonry walls subjected to blast loads. *International Journal of Computational Methods and Experimental Measurements*, **9**(4), pp. 296–308, 2021.
[12] Castedo, R., Santos, A.P., Alañón, A., Reifarth, C., Chiquito, M., López, L.M., Martínez-Almajano, S. & Pérez-Caldentey, A., Numerical study and experimental tests on full-scale RC slabs under close-in explosions. *Engineering Structures*, **231**, 111774, 2021.
[13] Ruggiero, A., Bonora, N., Curiale, G., De Muro, S., Iannitti, G., Marfia, S., Sacco, E., Scafati, S. & Testa, G., Full scale experimental tests and numerical model validation of reinforced concrete slab subjected to direct contact explosion. *International Journal of Impact Engineering*, **132**, 103309, 2019.
[14] Draganić, H., Gazić, G. & Varevac, D., Experimental investigation of design and retrofit methods for blast load mitigation: A state-of-the-art review. *Engineering Structures*, **190**, pp. 189–209, 2019.
[15] Goswami, A. & Adhikary, S.D., Retrofitting materials for enhanced blast performance of Structures: Recent advancement and challenges ahead. *Construction and Building Materials*, **204**, pp. 224–243, 2019.
[16] Caldentey, A.P., Diego, Y.G., Fernández, F.A. & Santos, A.P., Testing robustness: A full-scale experimental test on a two-storey reinforced concrete frame with solid slabs. *Engineering Structures*, **240**, 112411, 2021.
[17] Bisyk, S.P., Chepkov, I.B., Vaskivskyy, M.I., Davydovskyi, L.S., Slyvinskyy, O.A. & Aristarkhov, O.M., Methods for modelling Air blast on structures in LS-DYNA. Comparison and analysis. *Weapons and Military Equipment*, **1**, pp. 22–31, 2019.
[18] Kingery, C. & Bulmash, G., Airblast parameters from TNT spherical air burst and hemispherical surface burst. US Army Armament and Development Center, Ballistic Research Laboratory, 1984.
[19] Reifarth, C., Castedo, R., Santos, A.P., Chiquito, M., López, L.M., Pérez-Caldentey, A., Martínez-Almajano, S. & Alañón, A., Numerical and experimental study of externally reinforced RC slabs using FRPs subjected to close-in blast loads. *International Journal of Impact Engineering*, **156**, 103939, 2021.
[20] Xiao, W., Andrae, M. & Gebbeken, N., Experimental and numerical investigations of shock wave attenuation effects using protective barriers made of steel posts. *Journal of Structural Engineering*, **144**(11), 04018204, 2018.
[21] Helal, J., Sofi, M. & Mendis, P., Non-destructive testing of concrete: A review of methods. *Electronic Journal of Structural Engineering*, **14**(1), pp. 97–105, 2015.
[22] López, L.M., Castedo, R., Chiquito, M., Segarra, P., Sanchidrián, J.A., Santos, A.P. & Navarro, J., Post-blast non-destructive damage assessment on full-scale structural elements. *Journal of Nondestructive Evaluation*, **38**(1), pp. 1–15, 2019.
[23] UFC 3-340-02, Structures to resist the effects of accidental explosions. US Department of the Army, Navy and Air Force Technical Manual, 2008.
[24] Chiquito, M., Castedo, R., López, L.M., Santos, A.P., Mancilla, J.M. & Yenes, J.I., Blast wave characteristics and TNT equivalent of improvised explosive device at small scaled distances. *Defence Science Journal*, **69**(4), pp. 328–335, 2019.

[25] UNE-EN 1992-1-1:2013: Eurocode 2: Design of concrete structures – Part 1-1: General rules and rules for buildings, 2013.

[26] Alañón, A., Cerro-Prada, E., Vázquez-Gallo, M.J. & Santos, A.P., Mesh size effect on finite-element modeling of blast-loaded reinforced concrete slab. *Engineering with Computers*, **34**(4), pp. 649–658, 2018.

[27] Murray, Y.D., User's manual for LS-DYNA concrete material model 159 (No. FHWA-HRT-05-062). Federal Highway Administration. Office of Research, Development, and Technology, USA, 2007.

[28] Livermore Software Technology Corporation (LSTC). LS-DYNA Keyword User's Manual – R11 2018:3186.

[29] Malvar, L.J., Crawford, J.E., Wesevich, J.W. & Simons, D., A plasticity concrete material model for DYNA3D. *International Journal of Impact Engineering*, **19**(9–10), pp. 847–873, 1997.

[30] Castedo, R., Segarra, P., Alañón, A., Lopez, L.M., Santos, A.P. & Sanchidrián, J.A., Air blast resistance of full-scale slabs with different compositions: Numerical modeling and field validation. *International Journal of Impact Engineering*, **86**, pp. 145–156, 2015.

[31] Hashin, Z., Failure criteria for unidirectional fiber composites. *Journal of Applied Mechanics*, **180**, pp. 329–334, 1980.